Characterizing Errors in MRMS Quantitative Precipitation Estimates Over Alaska, Hawaii, and Puerto Rico

EMILIA THEDENS*

National Weather Center Research Experiences for Undergraduates Program
Norman, Oklahoma

ROBERT A. CLARK III

NOAA/OAR/National Severe Storms Laboratory
Norman, Oklahoma

HEATHER GRAMS

NOAA/OAR/National Severe Storms Laboratory
Norman, Oklahoma

STEVEN M. MARTINAITIS

Cooperative Institute for Mesoscale Meteorological Studies
The University of Oklahoma
NOAA/OAR National Severe Storms Laboratory
Norman, Oklahoma

ABSTRACT

Four radar-based quantitative precipitation estimation (QPE) products from the Multi-Radar Multi-Sensor (MRMS) system are evaluated against hourly and daily gauge-based rainfall amounts over Alaska, Hawaii, and Puerto Rico. Three products are 1) Radar-Only QPE (Q3RAD), the initial version of MRMS QPE that is reflectivity-based, 2) Dual-Polarization QPE (Q3DP), a version of Q3RAD which uses dual-polarization variables in its calculations, 3) Dual-Polarization QPE with Evaporation Correction (Q3EVAP), a product which adds an evaporation correction to Q3DP, and 4) Multi-Sensor QPE (Q3MS), which utilizes gauge-based correction and terrain data and is evaluated daily. The evaluation of QPE data takes place from June 2019 to June 2021. Both the Alaska and Puerto Rico domains exhibited spatial error trends corresponding to the quality of radar coverage, with larger errors in regions of poor coverage. The Hawaii domain was characterized by underestimation throughout the region. Puerto Rico was prone to overestimates in the west, but did not have a problem with underestimation. The results of the study are useful to those who wish to learn more about the present limitations and challenges of radar-based QPE in domains outside the continental United States.

1. Introduction

Accurate and timely quantitative precipitation estimates (QPEs) are vital to real-time flash flood modeling, agriculture, and water resource management. Creating a QPE system which yields precise estimates at a high spatial-temporal resolution, however, is a challenge. There are two primary approaches to QPE derived from different sources: rain gauge-based QPE and remotely sensed QPE. Both have specific advantages and drawbacks.

Rain gauges provide relatively accurate rainfall measurements, but those measurements are confined to the single gauge point. Rain gauges lack the spatial distribution necessary to accurately represent highly variable precipitation events (e.g. Kitchen and Blackall 1992, Goodrich et al. 1995) and are too sparse for some hydrological applications (e.g. Sempere-Torres et al. 1999). Individual points of gauge data have limits in their accuracy. These limitations include bias due to a poor gauge site (Sieck et al. 2007), undercatch due to surface wind (e.g., Larson and Peck 1974; Pollock et al. 2018), blockage of the gauge opening (Sieck et al. 2007), and bias due to mechanical instrumentation impairment (Martinaitis et al. 2015).

*Corresponding author address: Emilia Thedens, Luther College, 400 College Dr., Decorah, IA
E-mail: emiliathedens@gmail.com

Precipitation melt and/or stuck gauges can compromise precipitation measurements in scenarios with solid winter snow (Qi et al. 2016). Solid winter precipitation increases the size of undercatch due to wind (Goodison and Yang 1998; Nešpor and Sevruk 1999). Strong winds, instrumentation breakdown, and winter freezing can result in entirely compromised or missing data (e.g. Qi et al. 2016; Martinaitis et al. 2015).

Radar-based QPE can be generated at a high spatial-temporal resolution, and can therefore better represent the variability of precipitation (Berne and Krajewski 2013). But radar-based QPE does still have drawbacks, including errors in areas with poor radar coverage and other biases (Zhang et al. 2020). Possible sources of this error includes the presence of a large part of the radar beam intersecting the melting layer (which causes bright band contamination), the presence of hail, and partial or full blockage of the radar beam by terrain or physical objects (Austin 1987; Andrieu et al. 1997). In recent years, there have been many notable advancements in radar-based QPE incorporated into the Multi-Radar Multi-Sensor (MRMS) suite of products developed by the NOAA National Severe Storms Laboratory (NSSL) (Zhang et al. 2016). Among these are the precipitation classification capabilities of dual-polarization radar (Park et al. 2009) and schemes to mitigate clutter and bright band contamination.

The drawbacks of radar-based QPE are evident in the MRMS domains outside the continental United States (OCONUS domains). Areas in northern Alaska are completely uncovered by radar; additionally, in Alaska, Hawaii, and Puerto Rico, mountainous terrain contributes to significant beam blockage (Fig. 1). Despite its drawbacks, radar-based QPE's higher spatial-temporal resolution necessitates its use in these regions. Alaska, Hawaii, and Puerto Rico are all susceptible to floods (O'Connor and Costa 2004), which demonstrates the urgent need for remote sensing and fast detection of precipitation in these regions. While MRMS products are operational in the OCONUS domains, their errors in these areas have not been systematically investigated. The purpose of this study is to examine and quantify the error characteristics of MRMS QPE products over Alaska, Hawaii, and Puerto Rico.

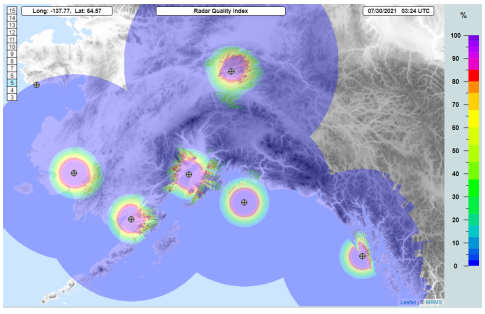

(a)

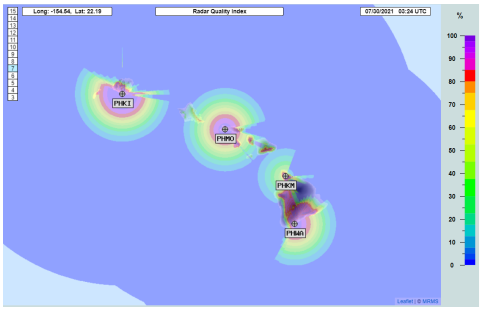

(b)

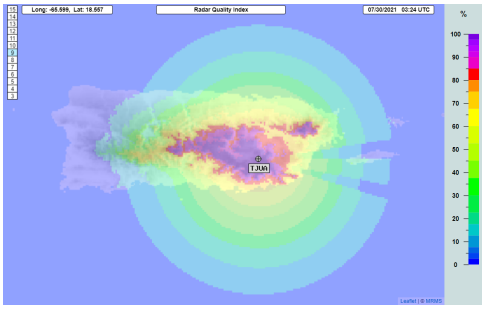

(c)

FIG. 1: Radar Quality Index (RQI) product-viewer for Alaska (a), Hawaii (b), and Puerto Rico (c). Includes overlay of radar locations and is shaded topographically.

2. Data

The data for this study are from June 2019 to June 2021 and include MRMS QPEs, rain gauge measurements, location data, Numerical Weather Prediction (NWP) fields, and PRISM. QPE data analyses are hourly for Q3RAD, Q3DP, and Q3EVAP. The QPE data analysis for Q3MS uses 24-h accumulations. The analyses of each product are conducted over three domains: Alaska, Hawaii, and the Caribbean. Each domain area is bounded by latitude/longitude coordinates (Table 1).

TABLE 1: OCONUS Domain Boundaries for MRMS Products

Domain	*Latitude*	*Longitude*
Alaska	$50°N$ to $72°N$	$176°W$ to $126°W$
Hawaii	$15°N$ to $26°N$	$164°W$ to $151°W$
Caribbean	$10°N$ to $25°N$	$91°W$ to $60°W$

a. MRMS QPE Products

The authors used four MRMS QPE products in this study. These products are as follows:

- Radar-Only QPE (Q3RAD)
- Dual-Polarization QPE (Q3DP)
- Dual-Polarization QPE with Evaporation Correction (Q3EVAP)
- Multi-Sensor QPE (Q3MS)

Q3RAD uses both the precipitation classification capabilities of dual-pol radar and the clutter and bright band filtration schemes described previously for its estimations. Quality-controlled radar data are transformed into a precipitation quantity at each grid cell through a unique reflectivity-rain rate relationship ($R-Z$) based on a surface precipitation classification scheme (Zhang et al. 2016). Hydrometeors are classified by a set of parameters which includes data from the Rapid Refresh (RAP) numerical weather prediction model in Hawaii and Puerto Rico, and the High Resolution Rapid Refresh (HRRR) model in Alaska.

Q3DP differs from Q3RAD in that it uses dual-polarization moments to estimate precipitation rates; this includes specific differential phase (K_{dp}) in areas with potential hail and specific attenuation estimation (A) in areas of pure rain (Zhang et al. 2020). Using the specific attenuation-rate rate relationship ($R-A$), the K_{dp}-rain rate relationship ($R-K_{dp}$), and $R-Z$ above the melting layer, a synthetic rain rate estimate is formed (Zhang et al. 2020). Evaluation of Q3DP has shown that it has less errors than Q3RAD across the CONUS; specifically, Q3DP reduces the heavy rainfall wet bias and underestimation in areas with partial beam blockage (Zhang et al. 2020). However, these evaluations also show that Q3DP tends to underestimate cases with light rain, especially in regions where there is beam blockage (Zhang et al. 2020).

Q3EVAP applies an evaporation correction scheme to Q3DP (Martinaitis et al. 2018). This evaporation correction is designed to account for the portion of precipitation which evaporates before it reaches the surface. First, 3D RAP data are used to create an environmental profile. Then an evaporation correction based on precipitation type is applied at several levels in that 3D profile until it reaches the surface. Q3EVAP corrects some overestimation, but can worsen underestimation, especially in cases where radar quality is low (Zhang et al. 2020). In cases where the radar beam height is high (and RQI is therefore low), the evaporation correction can worsen underestimates from overshooting.

Q3MS applies a local gauge-based correction (LGC) scheme to radar estimations, while Mountain Mapper QPE (MM; Zhang et al. 2016) and model QPF are used to fill in radar coverage gaps (Martinaitis et al. 2020). MM interpolates gauge observations onto orthographic data from the Parameter-Elevation Regressions on Independent Slopes Model (PRISM; Daly et al. 2008, 1994). The model QPF data used are from the High-Resolution Rapid Refresh (HRRR) model (Benjamin et al. 2016) . The gauge data used in MM and the LGC radar estimates are from the Hydrometeorological Automated Data System (HADS; Kim et al. 2009) and the Meteorological Assimilation Data Ingest System (MADIS; Helms et al. 2019). Gauge data go through a quality control algorithm (Martinaitis et al. 2021). Estimates from multi-sensor QPE have shown improvement over MRMS radar-only QPE in areas of the western CONUS where beam blockage is a challenge (Martinaitis et al. 2020).

b. Supplementary Data

Radar Quality Index (RQI) is a MRMS product based on a beam blockage component and a component determined by variation in the vertical profile of reflectivity. RQI is defined on a scale from 0 to 1, where 1 indicates high radar quality and a radar beam entirely below the melting layer (Zhang et al. 2016). Low RQI has been shown to be associated with radar QPE errors (Chen 2013).

c. Gauge Data

For this study, the authors considered gauge data as ground truth. Gauge data compared to the Q3RAD, Q3DP, and Q3EVAP products are from the HADS and MADIS networks.The Q3MS gauge-adjustment process utilizes the HADS and MADIS gauge data that passed the MRMS gauge quality control logic; thus the authors used 24-hour gauge data from the Community Collaborative Rain, Hail, and Snow (CoCoRaHS) Network for independent evaluations of Q3MS. The Q3MS gauge-adjustment process utilizes MADIS gauge data.

3. Methodology

The methodology for this study was inspired by Chen (2013) and extends the work of Santer and Grams (2021).

a. Data Filtering and Compilation

The authors used data from a long term archive of MRMS QPE data for the OCONUS domain evaluations. QPEs were matched to gauge observations. The hourly HADS and MADIS gauge data were filtered through the quality control algorithm described in Martinaitis et al. (2021). The authors used gauge data which passed or conditionally passed the quality test according to the MRMS flags. Gauge data which has been entirely removed from the data set due to MRMS flags include suspect values that are considered unrealistic, outlier values when compared to radar data, and false values when compared to QPE sources. MRMS flags also filter most cases where Q3DP or the gauge differ on the presence of precipitation; there are some exceptions in which the gauge is on the

edge of a precipitation area. MRMS flags gauge measurements which have a corresponding RQI which is less than 0.4 as a conditional pass in most cases. In addition to filtering data through the quality control algorithm, the authors themselves filtered out data where radar precipitation is missing and data where all three QPEs were zero.

b. Statistical Methods

The authors were primarily concerned with two attributes of MRMS product errors: size and bias. There are three error statistics that the authors used to characterize these two attributes: mean accumulated difference (MAD), root squared mean error (RMSE), and Pearson's correlation coefficient (PCC),

$$MAD = \frac{\sum_{i=1}^{N} E_i - G_i}{N}. \tag{1}$$

$$RMSE = \sqrt{\frac{\sum_{i=1}^{N} (E_i - G_i)^2}{N}}. \tag{2}$$

$$PCC = \frac{\sum_{i=1}^{N} (E_i - \tilde{E})(G_i - \tilde{G})}{\sqrt{\sum_{i=1}^{N} (E_i - \tilde{E})^2 \sum_{i=1}^{N} (G_i - \tilde{G})^2}}. \tag{3}$$

where E_i denotes the ith rainfall estimation, G_i denotes the ith gauge observation, and N denotes the total number of observations. The authors used MAD to evaluate QPE bias and RMSE and PCC to evaluate QPE accuracy. To evaluate correlations and interaction effects, the authors binned the data by location, by environmental parameters, and by gauge accumulation.

4. Results

Many individual points have few observations; the authors masked grid points with less than 15 observations in geographical graphs as there were too few observations to robustly represent the area.

a. Alaska

Q3EVAP tends to underestimate precipitation in the Alaska panhandle (Fig. 2a). There is slight overestimation around Anchorage and on the southern edge of the Cook Inlet, but slight underestimation on the oceanic side of Cook Inlet. In general, there is dry-bias over portions of Alaska (Fig. 2a).

The highest RMSE is on the eastern side of Alaska, though there is another small cluster slightly west of the Cook Inlet (Fig. 2b). While RQI is near 0 around the Cook Inlet (Fig. 1a), RMSE is between 1 and 2 mm which is comparable to that over much of CONUS (Santer and Grams 2021). PCC is lower north of the Cook Inlet and in spots between the Fairbanks and Anchorage clusters (Fig. 2c).

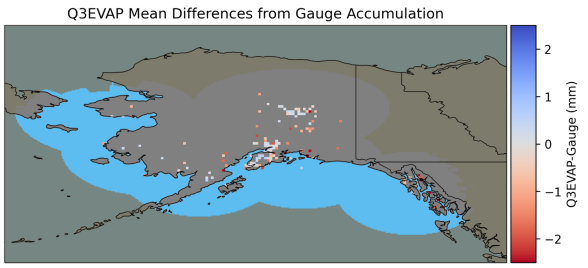

(a)

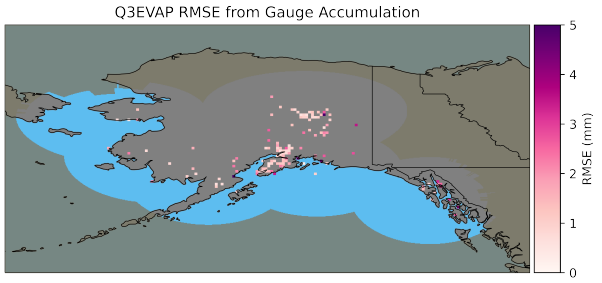

(b)

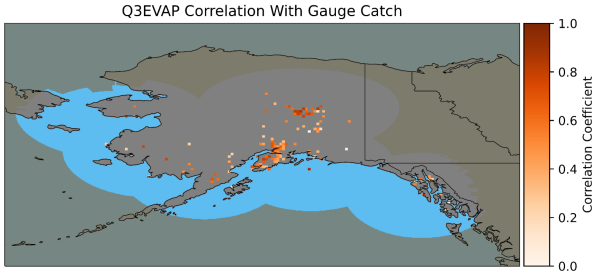

(c)

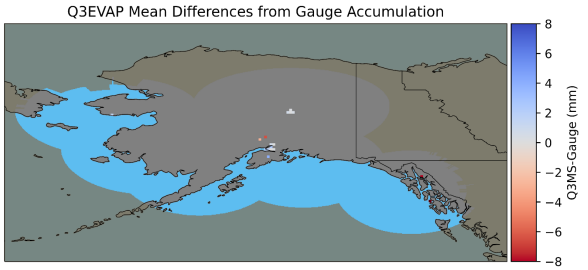

(d)

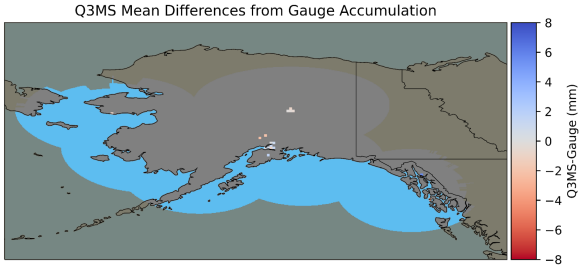

(e)

FIG. 2: MAD (a), RMSE (b), and PCC (c) values for Q3EVAP over Alaska; MAD for QEVAP 24-h data (d) and Q3MS 24-h data (e). Square size is approximately 100 km^2.

Q3MS has less bias than Q3EVAP for the 24-h data, with the caveat that the range of CoCoRaHS data over Alaska is very limited (Fig. 2d - 2e).

(Fig 2c).

At high levels of gauge accumulation, a large portion of the rain is undetected (Fig. 3a). Cases with high RQI tend to have errors closer to zero, though data for large rain amounts in high RQI areas is limited in Alaska (Fig 3b). Though the data for large rain amounts is limited, this suggests that large volumes of rain are undetected with lower RQI and confirms previous analysis of MRMS QPE products (Santer and Grams 2021). Q3RAD has a larger tendency towards overestimation with high RQI (Fig 3b; Q3EVAP and Q3DP are almost identical (Fig. 3b), which suggests this is due to Q3DP's use of $R-A$ and not due to the evaporation connection in Q3EVAP; however, there is no direct relationship between RQI and error (Fig 3c).

b. Hawaii

Underestimation relative to gauges is prevalent throughout the state of Hawaii with the strongest average underestimation occurring on the north side of Kauai, the northeastern edge of Hawaii Island, and the central western coast of Hawaii Island. The island of Oahu and the southern portion of Kauai also suffer from underestimation, but to a lesser degree than elsewhere (Fig. 4a). The RQI map for the state of Hawaii depicts significant beam blockage over the northern part of Kauai (Fig. 1b), which does seem to line up with the location of the greatest underestimates, but the western portion of Oahu also has low RQI (Fig. 1b) with no such underestimates (Fig 4a).

The highest RMSE can be found on the north side of Kauai, the western portion of Oahu, the northeastern portion of Hawaii Island, and the central western edge of Hawaii Island (Fig. 4b). Overall, Hawaii Island and Maui tend to have higher RMSE than Oahu and Kauai (Fig. 4b. The western side of Kauai (which has lower RQI; Fig. 1b) did not have a strong bias but it does have a larger RMSE (Fig. 4b).

PCC is fairly consistent throughout the Hawaiian Islands. The southern and more interior portion of Hawaii Island tends to have higher correlation than the coast; the PCC is especially low at the interior of the western clump seen in the MAD and RMSE analysis (Fig. 4c). Correlation does not seem to differ across Kauai (Fig 4c); it is slightly lower on the northern edge of Oahu but this difference seems less pronounced than it was with MAD. Q3MS has lower RSME than Q3EVAP for the 24-h data in some locations (Fig. 4d -4e).

Most of the error charts for Hawaii did not seem to have much linearity, with two exceptions. There seems to be a fairly linear relationship (a negative correlation) between gauge catch and error (Fig. 5a). Q3EVAP and Q3DP have a bit more variability and are closer to zero. This suggests that the $R-A$ relationship used in Q3EVAP and Q3DP is less associated with underestimates in Hawaii. The other notable error chart is for the relationship between surface temperature (TSFC) and QPE-gauge differences. For all three MRMS radar-only products, underestimation is worst when TSFC is between 10 and 15 deg C but is reduced as temperatures rise (Fig. 3b).

c. Puerto Rico

Bias in Puerto Rico is variable over most of the region except on the western edge of the island, where there is consistent underestimation (Fig. 6a). Overestimates are less frequent and are more concentrated along the southern coastline (Fig. 6a). RMSE increases from east to west in Puerto Rico (Fig. 6b). It is highest on the western edge where RQI is also much lower (Fig. 1c). PCC is lower on the western edge of Puerto Rico (Fig. 6c).

5. Discussion and Conclusions

The negative correlation between gauge accumulation and error was observed with varying intensity and confidence in all three OCONUS domains. This negative correlation was also observed in CONUS (Santer and Grams 2021) when examining the same statistic. Large gauge accumulations are rare, and these plots do emphasize cases with medium to high gauge accumulations. A case with a gauge accumulation of 60 mm with Q3EVAP estimates of 30 mm might have a 50 percent detection rate but a 30 mm error. Operating with percent error creates a similar problem for areas with tinier amounts of rain. Despite these biases, the negative correlation between gauge accumulation and error is still important to consider.

Hawaii had significant underestimates for all three radar-based products. Error also tended to be fairly geographically concentrated, suggesting that these underestimates may be related to location. Hawaii is transitioning from RAP to HRRR currently; the improved resolution and accuracy expected in this upgrade will likely improve Q3MS estimates significantly.

Though RQI never had an explicit correlation with errors, the two still seem to be connected. The western edge of Puerto Rico had the highest RMSE values and is where there is the lowest RQI. Estimates in Hawaii also had more error around regions that had lower RQI. The interaction between RQI and the gauge-catch error relationship in Alaska suggests that RQI may interact with other variables. It is also possible that RQI is correlated with another unknown variable or geographic factor that contributes to the connection.

In 24 hour comparisons, Q3MS outperformed Q3EVAP in both Alaska and Hawaii. The locations of Q3MS analysis were highly restricted for Alaska. Little data exists as to how Q3MS estimates compare to Q3EVAP estimates in areas of Alaska with lower RQI. Hawaii's Q3MS data

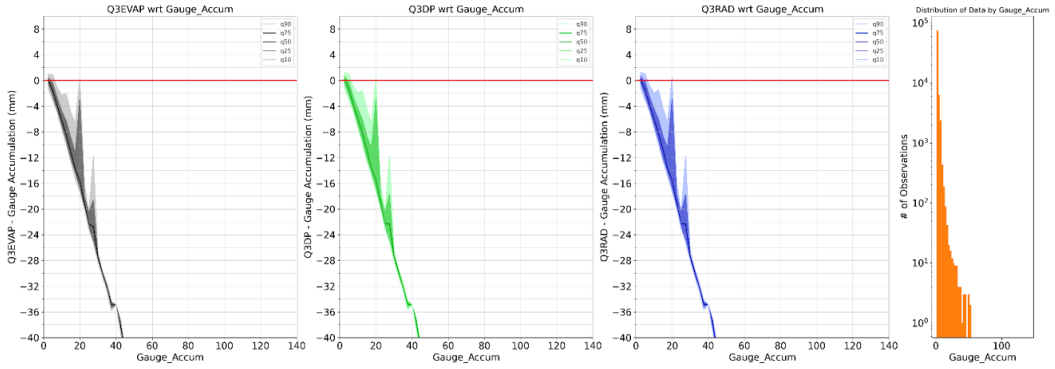

(a)

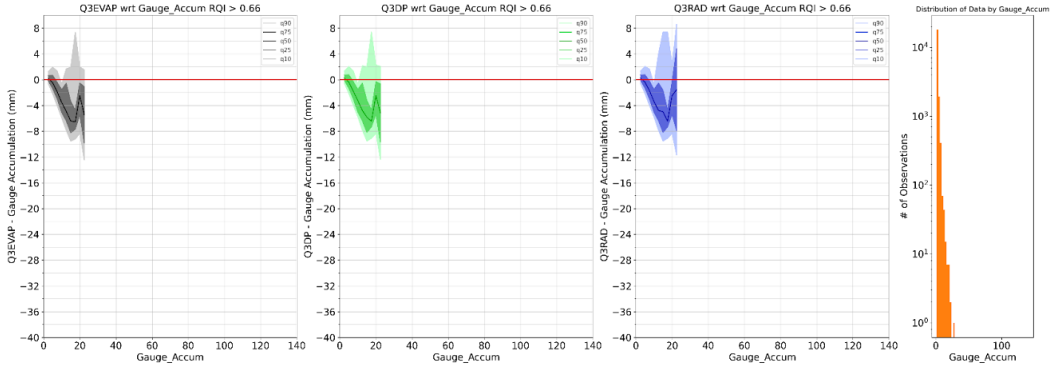

(b)

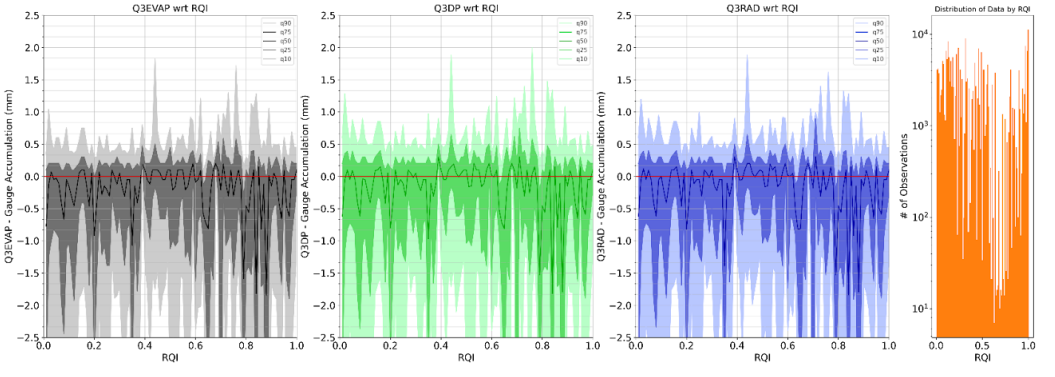

(c)

FIG. 3: Residual quantile plots for Q3RAD, Q3DP, and Q3EVAP in Alaska with respect to gauge accumulation (a), gauge accumulation with RQI > 0.66 (b), and RQI (c).

does include some areas with low RQI and does show improvement in some of those areas, but that may not be true for Alaska. Q3MS has the ability to cover a much wider area like Alaska than solely radar-based products, but fur-

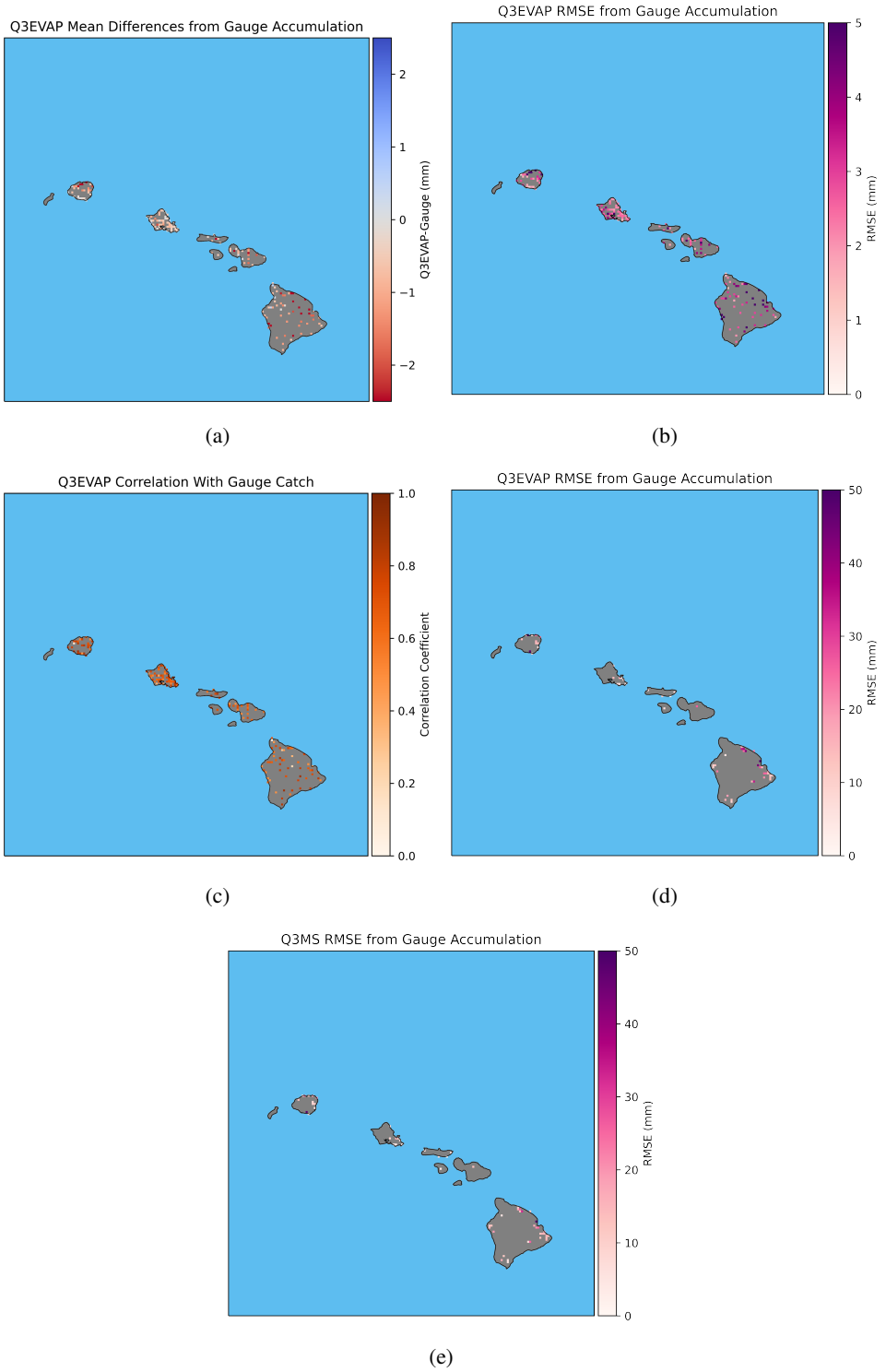

FIG. 4: MAD (a), RMSE (b), and PCC (c) for Q3EVAP over Hawaii. MAD for QEVAP 24-h data (d) and Q3MS 24-h data (e). Each square is about 20 km^2.

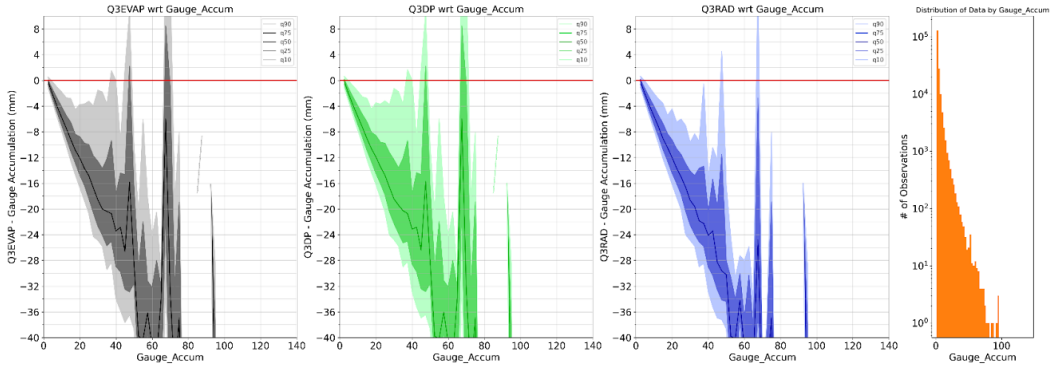

(a)

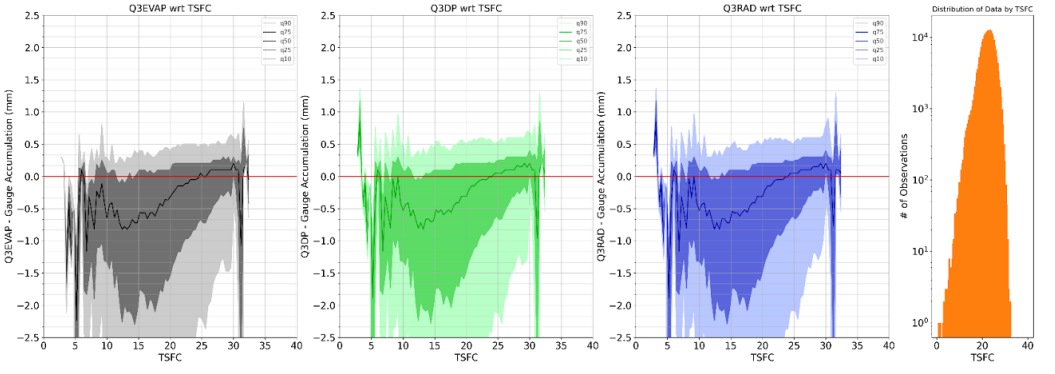

(b)

FIG. 5: Residual quantile plots for Q3RAD, Q3DP, and Q3EVAP in Hawaii with respect to gauge accumulation (a), surface temperature (TSFC; b).

ther analysis is needed to understand the uncertainty in the gaps filled by Q3MS.

Alaska faces the largest challenges when it comes to QPE. It is plagued by a lack of radar coverage, an issue which is not easily (or cheaply) fixed. Q3MS fills those gaps, but there is not enough independent CoCoRaHS data to properly evaluate its performance. Alaska also lacks widespread gauge data of a high enough quality to pass MRMS QC in many locations. Improving the quality of gauge data in these locations through improved instrument maintenance and siting would facilitate more thorough evaluations of QPE products in Alaska and may ensure more accurate gap-filling QPE from Q3MS. Alaska may benefit from satellite-based QPE.

Acknowledgments. The authors are grateful for funding for this work provided by National Science Foundation Grant No. AGS-2050267. We thank Dr. Micheal Simpson for his work compiling the dataset, and Henry Santer for sharing his Python work. We also extend special thanks to Daphne La Due and Alex Marmo for their leadership and direction during the 2021 National Weather Center Research Experience for Undergrads program and to Amanda Kis for her guidance in scientific writing.

References

Andrieu, H., J. Creutin, G. Delrieu, and D. Faure, 1997: Use of a weather radar for the hydrology of a mountainous area. part i: Radar measurement interpretation. *Journal of Hydrology*, **193**, 1–25, doi:10.1016/S0022-1694(96)03202-7.

Austin, P. M., 1987: Relation between measured radar reflectivity and surface rainfall. *Monthly Weather Review*, **115 (5)**, 1053 – 1070, doi:10.1175/1520-0493(1987)115⟨1053:RBMRRA⟩2.0.CO;2, URL https://journals.ametsoc.org/view/journals/mwre/115/5/1520-0493_1987_115_1053_rbmrra_2_0_co_2.xml.

Benjamin, S. G., and Coauthors, 2016: A north american hourly assimilation and model forecast cycle: The Rapid Refresh. *Monthly Weather Review*, **144 (4)**, 1669 – 1694, doi:10.

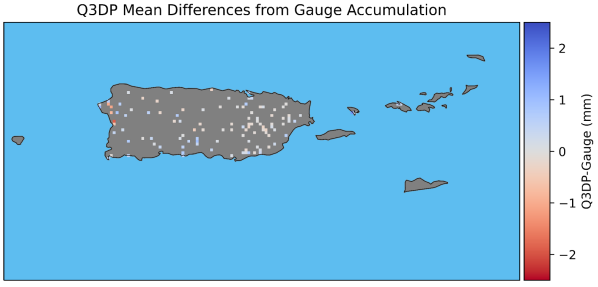

(a)

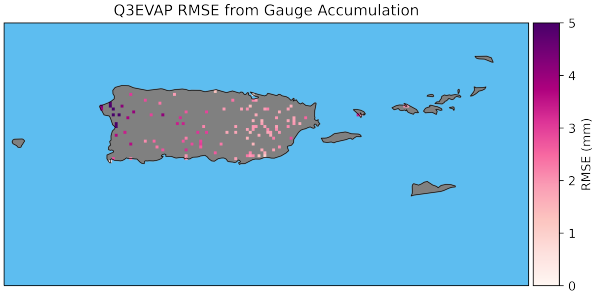

(b)

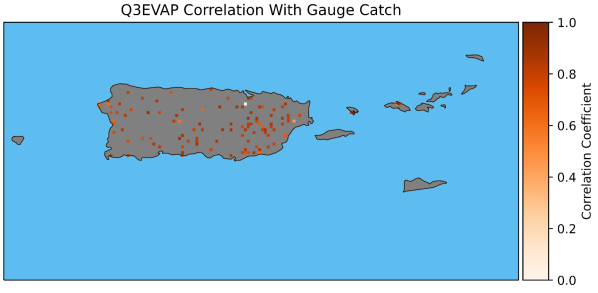

(c)

FIG. 6: MAD (a), RMSE (b), and PCC (c) values for Q3EVAP over Puerto Rico. Square size is approximately 3 km^2.

1175/MWR-D-15-0242.1, URL https://journals.ametsoc.org/view/journals/mwre/144/4/mwr-d-15-0242.1.xml.

Berne, A., and W. Krajewski, 2013: Radar for hydrology: Unfulfilled promise or unrecognized potential? *Advances in Water Resources*, **51**, 357–366, doi:10.1016/j.advwatres.2012.05.005.

Chen, S., 2013: Evaluation and uncertainty estimation of NOAA/NSSL next-generation National Mosaic QPE (Q2) over the continental united states. *J. Hydrometeor.*, **14**, 1308–1322.

Daly, C., M. Halbleib, J. I. Smith, W. P. Gibson, M. K. Doggett, G. H. Taylor, J. Curtis, and P. P. Pasteris, 2008: Physiographically sensitive mapping of climatological temperature and precipitation across the conterminous united states. *International Journal of Climatology*, **28 (15)**, 2031–2064, doi:https://doi.org/10.1002/joc.1688, URL https://rmets.onlinelibrary.wiley.com/doi/abs/10.1002/joc.1688, https://rmets.onlinelibrary.wiley.com/doi/pdf/10.1002/joc.1688.

Daly, C., R. P. Neilson, and D. L. Phillips, 1994: A statistical-topographic model for mapping climatological precipitation over mountainous terrain. *Journal of Applied Meteorology and Climatology*, **33 (2)**, 140 – 158, doi:10.1175/1520-0450(1994)033⟨0140:ASTMFM⟩2.0.CO;2, URL https://journals.ametsoc.org/view/journals/apme/33/2/1520-0450_1994_033_0140_astmfm_2_0_co_2.xml.

Goodison, B. P. Y. T. L., B. E., and D. Yang, 1998: Wmo solid precipitation measurement intercomparison final report. Tech. Rep. Word Meteorological Organization Instruments and Observing Methods Report No. 67, Word Meteorological Organization, Geneva.

Goodrich, D. C., J.-M. Faurès, D. A. Woolhiser, L. J. Lane, and S. Sorooshian, 1995: Measurement and analysis of small-scale convective storm rainfall variability. *Journal of Hydrology*, **173 (1)**, 283–308, doi:https://doi.org/10.1016/0022-1694(95)02703-R, URL https://www.sciencedirect.com/science/article/pii/002216949502703R.

Helms, D., P. Miller, M. Barth, B. Starosta, B. Gordon, S. Schofield, F. Kelly, and S. Koch, 2019: Status update of the transition from research to operations of the meteorological assimilation data ingest system (madis). AZ.

Kim, D., B. Nelson, and D.-J. Seo, 2009: Characteristics of reprocessed Hydrometeorological Automated Data System (HADS) hourly precipitation data. *Weather and Forecasting*, **24 (5)**, 1287 – 1296, doi:10.1175/2009WAF2222227.1, URL https://journals.ametsoc.org/view/journals/wefo/24/5/2009waf2222227_1.xml.

Kitchen, M., and R. Blackall, 1992: Representativeness errors in comparisons between radar and gauge measurements of rainfall. *Journal of Hydrology*, **134 (1)**, 13–33, doi:https://doi.org/10.1016/0022-1694(92)90026-R, URL https://www.sciencedirect.com/science/article/pii/002216949290026R.

Larson, L. W., and E. L. Peck, 1974: Accuracy of precipitation measurements for hydrologic modeling. *Water Resources Research*, **10 (4)**, 857–863, doi:https://doi.org/10.1029/WR010i004p00857, URL https://agupubs.onlinelibrary.wiley.com/doi/abs/10.1029/WR010i004p00857, https://agupubs.onlinelibrary.wiley.com/doi/pdf/10.1029/WR010i004p00857.

Martinaitis, S. M., S. B. Cocks, Y. Qi, B. T. Kaney, J. Zhang, and K. Howard, 2015: Understanding winter precipitation impacts on automated gauge observations within a real-time system. *J. Hydrometeor.*, **16**, 2345–2363.

Martinaitis, S. M., S. B. Cocks, M. J. Simpson, A. P. Osborne, S. S. Harkema, H. M. Grams, J. Zhang, and K. W. Howard, 2021: Advancements and characteristics of gauge ingest and quality control within the multi-radar multi-sensor system. *Journal of Hydrometeorology*, doi:10.1175/JHM-D-20-0234.1, URL https://journals.ametsoc.org/view/journals/hydr/aop/JHM-D-20-0234.1/JHM-D-20-0234.1.xml.

Martinaitis, S. M., H. M. Grams, C. Langston, J. Zhang, and K. Howard, 2018: A real-time evaporation correction scheme for radar-derived mosaicked precipitation estimations. *Journal of Hydrometeorology*, **19 (1)**, 87 – 111, doi:10.1175/JHM-D-17-0093.1, URL https://journals.ametsoc.org/view/journals/hydr/19/1/jhm-d-17-0093_1.xml.

Martinaitis, S. M., and Coauthors, 2020: A physically based multi-sensor quantitative precipitation estimation approach for gap-filling

radar coverage. *Journal of Hydrometeorology*, **21 (7)**, 1485 – 1511, doi:10.1175/JHM-D-19-0264.1, URL https://journals.ametsoc.org/view/journals/hydr/21/7/jhmD190264.xml.

Nešpor, V., and B. Sevruk, 1999: Estimation of wind-induced error of rainfall gauge measurements using a numerical simulation. *Journal of Atmospheric and Oceanic Technology*, **16 (4)**, 450 – 464, doi:10.1175/1520-0426(1999)016⟨0450:EOWIEO⟩2.0.CO;2, URL https://journals.ametsoc.org/view/journals/atot/16/4/1520-0426_1999_016_0450_eowieo_2_0_co_2.xml.

O'Connor, J. E., and J. E. Costa, 2004: Spatial distribution of the largest rainfall-runoff floods from basins between 2.6 and 26,000 km2 in the united states and puerto rico. *Water Resources Research*, **40 (1)**, doi:https://doi.org/10.1029/2003WR002247, URL https://agupubs.onlinelibrary.wiley.com/doi/abs/10.1029/2003WR002247, https://agupubs.onlinelibrary.wiley.com/doi/pdf/10.1029/2003WR002247.

Park, H. S., A. V. Ryzhkov, and D. S. Zrnic, 2009: The hydrometeor classification algorithm for the polarimetric wsr-88d: Description and application to an mcs. *Wea. Forecasting*, **24**, 730–748.

Pollock, M. D., and Coauthors, 2018: Quantifying and mitigating wind-induced undercatch in rainfall measurements. *Water Resources Research*, **54 (6)**, 3863–3875, doi:https://doi.org/10.1029/2017WR022421, URL https://agupubs.onlinelibrary.wiley.com/doi/abs/10.1029/2017WR022421, https://agupubs.onlinelibrary.wiley.com/doi/pdf/10.1029/2017WR022421.

Qi, Y., S. Martinaitis, J. Zhang, and S. Cocks, 2016: A real-time automated quality control of hourly rain gauge data based on multiple sensors in MRMS system. *Journal of Hydrometeorology*, **17 (6)**, 1675 – 1691, doi:10.1175/JHM-D-15-0188.1, URL https://journals.ametsoc.org/view/journals/hydr/17/6/jhm-d-15-0188_1.xml.

Santer, H., and H. Grams, 2021: Evaluation and uncertainty of MRMS v12 dual-polarized radar quantitative estimation products. *35th Conference on Hydrology, Amer. Meteor. Soc.*, URL https://ams.confex.com/ams/101ANNUAL/meetingapp.cgi/Paper/378151.

Sempere-Torres, D., C. Corral, J. Raso, and P. Malgrat, 1999: Use of weather radar for combined sewer overflows monitoring and control. *Journal of Environmental Engineering*, **125 (4)**, 372–380, doi:10.1061/(ASCE)0733-9372(1999)125:4(372).

Sieck, L. C., S. J. Burges, and M. Steiner, 2007: Challenges in obtaining reliable measurements of point rainfall. *Water Resources Research*, **43 (1)**, doi:https://doi.org/10.1029/2005WR004519, URL https://agupubs.onlinelibrary.wiley.com/doi/abs/10.1029/2005WR004519, https://agupubs.onlinelibrary.wiley.com/doi/pdf/10.1029/2005WR004519.

Zhang, J., L. Tang, S. Cocks, P. Zhang, A. Ryzhkov, K. Howard, C. Langston, and B. Kaney, 2020: A dual-polarization radar synthetic QPE for operations. *Journal of Hydrometeorology*, **21 (11)**, 2507 – 2521, doi:10.1175/JHM-D-19-0194.1, URL https://journals.ametsoc.org/view/journals/hydr/21/11/JHM-D-19-0194.1.xml.

Zhang, J., and Coauthors, 2016: Multi-Radar Multi-Sensor (MRMS) quantitative precipitation estimation: Initial operating capabilities. *Bulletin of the American Meteorological Society*, **97 (4)**, 621 – 638, doi:10.1175/BAMS-D-14-00174.1, URL https://journals.ametsoc.org/view/journals/bams/97/4/bams-d-14-00174.1.xml.